J Geod (2005) 79: 175–188
DOI 10.1007/s00190-005-0448-z

ORIGINAL ARTICLE

C. Brunini · A. Meza · W. Bosch

Temporal and spatial variability of the bias between TOPEX- and GPS-derived total electron content

Received: 9 April 2004 / Accepted: 21 February 2005 / Published online: 30 June 2005

Abstract Total electron content (TEC) predictions made with the GPS-based la plata ionospheric model (LPIM) and the International Reference Ionosphere (IRI95) model were compared to estimates from the dual-frequency altimeter onboard the TOPEX/Poseidon (T/P) satellite. LPIM and IRI95 were evaluated for the location and time of available T/P data, from January 1997 to December 1998. To investigate temporal and spatial variations of the TEC bias between T/P and each model, the region covered by T/P observations was divided into ten latitude bands. For both models and for all latitudes, the bias was mainly positive (i.e. T/P values were larger); the LPIM bias was lower and less variable than the IRI95 bias. To perform a detailed analysis of temporal and spatial variability of the T/P-LPIM TEC bias, the Earth's surface was divided into spherical triangles with 9°-sides, and a temporally varying regression model was fitted to every triangle. The highest TEC bias was found over the equatorial anomalies, which is attributed to errors in LPIM. A significant TEC bias was found at 40°N latitude, which is attributed to errors in the T/P Sea State Bias (SSB) correction. To separate systematic errors in the T/P TEC from those caused by LPIM, altimeter range biases estimated by other authors were analysed in connection with the TEC bias. This suggested that LPIM underestimates the TEC, particularly during the Southern Hemisphere summer, while T/P C-band SSB calibration is worse during the Southern Hemisphere winter.

Keywords Total electron content (TEC) · GPS · TOPEX/Poseidon

C. Brunini (✉) · A. Meza
Facultad de Ciencias Astronómicas y Geofísicas,
Universidad Nacional de La Plata and Consejo
Nacional de Investigaciones Científicas y Técnicas,
Paseo del Bosque S/N, B1900 FWA La Plata, Argentina
E-mail: claudio@fcaglp.unlp.edu.ar;
ameza@fcaglp.fcaglp.unlp.edu.ar

W. Bosch
Deutsches Geodaetisches Forschungsinstitut, Marstallplatz 8,
80539 München, Germany
E-mail: bosch@dgfi.badw.de

1 Introduction

Satellite beacon techniques based on dual-frequency observations have proven their usefulness for remotely sensing the Earth's ionosphere. The leading ionospheric parameter recovered from transionospheric dual-frequency signals is the total electron content (TEC), i.e. the electron density integrated along the entire path of a signal (e.g., Leitinger and Putz 1988). TEC is measured in total electron content units (TECU; 1 TECU being 10^{16} electrons/m^2). Depending on local time, solar activity, geomagnetic conditions, region of the Earth, etc., the vertical TEC varies from about 1 to 180 TECU. Over the last decade, both the global positioning system (GPS) and the TOPEX/Poseidon (T/P) mission played a key role in TEC studies. Nevertheless, the crucial problem to assess the reliability of both TEC estimates is still not completely understood.

Global positioning system satellites broadcast two signals at frequencies of 1.575 GHz (L1) and 1.228 GHz (L2). The sensitivity of the ionospheric range delay to the TEC for the L1 signal is 162 mm/TECU (Langley 1996). Hence, the range delay for this signal can reach as much as 90 m for a low elevation satellite. Errors in the GPS-derived vertical TEC arise from different problems (Manucci et al. 1999). GPS signals provide slant satellite-to-receiver TEC estimates that must be converted into vertical TEC. It involves approximations such as representing the whole ionosphere by a spherical layer of infinitesimal thickness, neglecting the horizontal gradients of the electron density distribution, etc. Moreover, GPS slant TEC estimates have to be calibrated, because they are contaminated by carrier-phase ambiguities and hardware biases in the satellites and receivers. In addition, the computation of vertical TEC global maps requires interpolation of the vertical TEC far away from the points where the GPS signals pierce the ionospheric shell.

Since 1992, T/P has provided precise estimates of sea-level height. T/P operates a primary signal in the K_U-band (13.6 GHz) and a secondary signal in the C-band (5.3 GHz) (Fu et al. 1994). It was the first dual-frequency altimeter, thus allowing an accurate correction for the ionospheric range

delay error and, as a by-product, a direct estimation of the TEC (Imel 1994). The sensitivity of the range delay to the TEC for the primary frequency is 2.2 mm/TECU. Hence, the range delay for this signal can vary from 2 cm to 40 cm. The precision of the K_U-band range delay correction is believed to be 1.1 cm (i.e., 5 TECU), in 1-s averages of T/P data (Zlotnicki 1994; Imel 1994). Because this error arises from instrumental noise, Imel (1994) and Zlotnicki (1994) recommend low-pass filtering the corrections over 15–25 successive measurements, thereby reducing the effects of noise by a factor of four to five.

It should be noted that the overall accuracy of the T/P range delay correction is more difficult to assess, because systematic errors may affect the correction. An error that would bias both the TEC and the sea-level height estimates is the Sea-State Bias (SSB) (Chelton et al. 2001), because of its frequency-dependent behaviour. Actually, the SSB correction is empirically estimated and assembles corrections for the electromagnetic and the skewness biases. The first arises because the power per unit surface area backscattered from wave troughs is greater than wave crests, thus biasing the measured sea-level toward wave troughs; the second accounts for the difference between the mean and the median scattering sea surfaces.

The problem of assessing the accuracy of different TEC estimates was addressed by comparing different estimates from different techniques. Several studies have found the T/P TEC to be greater than GPS-derived vertical TEC. This is a paradoxical result because GPS estimates are for the full ionosphere (Ciraolo and Spalla 1997), whereas T/P samples only the portion from the sea surface to the 1336-km altitude of the satellite. It is believed that above the T/P altitude, the plasmasphere adds a contribution that can be 10–20% of the TEC (Bilitza et al. 1999; Craven and Comfort 1988). This contribution is obviously not sampled by T/P, but it is also not well accounted for by the GPS vertical TEC derived from a single layer ionospheric model. Chelton et al. (2001) pointed out the possibility that this relative TEC bias indicates a systematic error in the T/P range correction.

Comparisons between T/P- and GPS-derived TEC are performed in the worst scenario for GPS, because GPS vertical TEC has to be interpolated far away from the observing sites. Over recent years, the global GPS tracking network has steadily expanded, but large oceanic areas are still uncovered. During the early period of the T/P mission, Christensen et al. (1994) found that GPS and T/P estimates of the K_U-band range correction agreed to better than 1 cm when T/P flew directly over GPS receivers. However, Imel (1994) found a global RMS difference between both TEC estimates of 8 cm, with the worst cases south of 35°S latitude, where the distribution of GPS receivers was very poor. Schreiner et al. (1997) estimated the ionospheric range correction along the T/P ground track by ingestion of GPS vertical TEC into the Parameterizsed Real-time Ionospheric Specification Model (PRISM) (Daniell et al. 1995). They found that the adjusted PRISM and the T/P TEC estimates were almost identical when the T/P ground track passed near a GPS station. However, a few hundred kilometres away from the piercing point of GPS measurements, discrepancies typically exceeded 2 cm, and were sometimes as large as 8 cm. Ho et al. (1997) and Manucci et al. (1998) arrived at a similar conclusion. They found an overall RMS difference between GPS and T/P derived TEC ranging from 5.8 TECU ($\approx$ 0.9-m range delay at the L1 frequency) within 100 km of a GPS station, to 12.5 TECU ($\approx$ 2-m range delay at the L1 frequency) at a distance of 4,000 km from a GPS station. Errors were larger in the equatorial region and Southern Hemisphere than in the middle- and high-latitudes of the Northern Hemisphere.

In recent times, Hernández-Pajares (2003) compared GPS-based vertical TEC and T/P TEC estimates. GPS TEC was computed by five different centres belonging to the International GPS Service (IGS) Ionospheric Working Group: Jet Propulsion Laboratory (JPL) (Manucci et al. 1998), European Space Agency (ESA) (Feltens 1998), Centre for Orbit Determination in Europe (CODE) (Schaer 1999), Universidad Politécnica de Cataluña (UPC) (Hernández-Pajares et al. 1999), and Energy Mines and Resources of Canada (EMR) (Gao et al. 1994). These centres used different algorithms, but almost the same database. The averaged T/P-GPS TEC biases and the corresponding standard deviations, all in TECU, were -1.0 ± 5.6 (JPL), $+3.1\pm9.1$ (ESA), $+1.4\pm6.5$ (CODE), $+0.8\pm5.6$ (UPC), and $+4.8\pm10.4$ (EMR). The biases showed a latitudinal dependence with extreme values of –4 and +16 TECU. This result also exemplifies the current consistency of GPS TEC.

Comparisons between T/P TEC and vertical TEC estimates from the DORIS (Doppler Orbitography and Radiopositioning Integrated by Satellite) system onboard the T/P satellite again showed systematically lower values for DORIS than T/P. Zlotnicki (1994) showed an example where DORIS ionospheric range corrections differed from T/P estimates by more than 2 cm over an along-track distance of more than 6,000 km. Moreover, he showed examples of 2–3 cm discrepancies over large geographical regions spanning entire ocean basins. Imel (1994) found that DORIS TEC was on average 4.5 TECU lower than T/P TEC. Codrescu et al. (2001) found a similar result.

In our previous paper (Meza et al. 2002), we performed a systematic comparison of GPS-derived TEC, the International Reference Ionosphere (IRI95) (Bilitza 1997) and the Bent model (Bent and Llewellyn 1973), with T/P estimates. To derive the GPS TEC, we used the La Plata Ionospheric Model (LPIM) (Brunini et al. 2003). Comparisons were performed on a global scale (within $\pm66°$ of latitude covered by T/P). We found systematic TEC biases of 2.5–3.0 TECU for T/P–LPIM, 1.7–3.0 TECU for T/P–IRI95 and 0.8–2.2 TECU for T/P–Bent. The biases were greater during equinox than during solstice periods. The current paper highlights a LPIM limitation to represent the vertical TEC in the equatorial anomaly region, which worsens for increasing solar activity. Problems in the T/P C-band SSB correction are also highlighted. We hope that this analysis yields a better insight into the individual contributions of both techniques to the relative TEC bias. In addition, any progress toward identifying a bias

in the T/P range correction can be useful not only for TEC but also for sea-level height studies.

2 TEC determinations

2.1 IRI and GPS-derived TEC

Semi-empirical ionospheric models like IRI (Bilitza 1997) are properly termed "climatologic", because they aim to predict average conditions and quasi-periodic variations, but they lack accuracy to describe the "weather of the day". Bilitza et al. (1999) assessed the accuracy of the IRI model using comparisons with GPS-derived vertical TEC. To better account for the plasmasphere contribution, a two-layer (instead of a single-layer) ionospheric model was adopted to derive the GPS vertical TEC. GPS data from all the available IGS (Beutler et al. 1999) stations were processed from 1991 to 1997 (more than half of the solar cycle), but the comparisons were restricted to quiet geomagnetic conditions. The agreement between the daily mean vertical TEC derived from GPS and IRI was 2 TECU, for TEC values lower than 20 TECU. For higher TEC values, they found larger discrepancies; up to 20 TECU and more. The GPS-derived vertical TEC was generally less than the IRI prediction.

To derive TEC from GPS data, we have used the LPIM (Brunini 1998; Brunini et al. 2003), which was validated by comparisons with other customary TEC estimates (Meza et al. 2002). The TEC is obtained using the so-called geometry-free linear combination of dual-frequency carrier-phase observations (e.g. Lanyi and Roth 1988). In a pre-processing stage, we reduce the ambiguities from the linear carrier-phase combination in a four-stage procedure: (1) time series of the geometry-free linear combination for every satellite-receiver pair are computed from both carrier-phase and P-code observations; (2) jumps in every carrier-phase time series are isolated and the data are grouped in continuous arcs; (3) a shift for every continuous arc is estimated, averaging the differences between carrier-phase and P-code data; (4) the shift is subtracted from the carrier-phase data. In this way, every continuous arc of carrier-phase observations is "levelled" (on average) to the P-code observations and the ambiguities are removed.

LPIM approaches the whole ionosphere by a spherical shell of infinitesimal thickness located 450 km above the Earth's surface (see Fig. 1). Signals coming from a satellite to a receiver pierce the shell at the so-called piercing point, where the zenith distance is z'. The slant TEC along the path of the signal is related to the vertical TEC at the piercing point by the approximate mapping function $\cos z'$. The two-dimensional vertical TEC distribution on the shell is described by a spherical harmonic expansion up to degree 12 and order 8, dependent on the solar-fixed longitude and [spherical] geographic latitude. The coefficients of the expansion are estimated by least squares using observations from the IGS global network. The observations are processed on a daily basis to simultaneously estimate: (1) a set of expansion coefficients for every 2-h UT interval [0–2), [2–4), . . . , [22–24); and (2) a daily calibration offset for each receiver and each satellite (the so-called differential code biases; Coco et al. 1991; Sardon and Zarraoa 1997). The estimated coefficients allow us to compute the vertical TEC for any location and time.

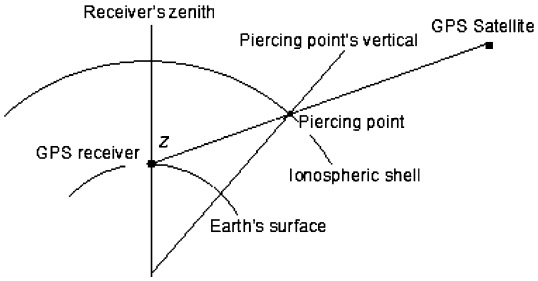

Fig. 1 Geometry of the infinitesimal-thickness spherical shell ionospheric model; the shell is 450 km above the Earth's surface (the figure is not to scale); a signal coming from a satellite arrives at a ground receiver with zenith angle z, and crosses the shell at the piercing point with zenith distance z'

Small circles in Fig. 2 show the location of the GPS receivers used in this research. The sites were selected to achieve a worldwide coverage as homogeneous as possible (a few representative stations were selected in USA, Europe and Japan). In spite of this, large data gaps over ocean regions were insurmountable. Increasing the maximum degree and order of the spherical harmonic expansion improves the representation of mesoscale TEC structures in those regions that are well covered by the GPS observations, but it can produce fictitious values over oceans and other regions poorly covered by the observations. The coverage of the observations (in the solar-fixed coordinate system) can be improved by increasing the length of the 2-h UT intervals, but it reduces the capability of LPIM to cope with temporal TEC variations. Therefore, it is necessary to find a compromise between the maximum degree and order of the expansion and the length of the UT intervals. Bearing in mind that we are going to compare LPIM and T/P TEC in ocean regions (i.e., far away from the GPS observing sites), we adopted a rather conservative compromise of maximum degree and order equal to 12 and 8 respectively and a time resolution of 2 h.

We assessed the accuracy of the LPIM vertical TEC by means of inter- and intra-technique comparisons. The results of inter-comparisons with IRI95 and Bent models, and with T/P estimates, were discussed by Meza et al. (2002), and have been briefly reviewed in the Introduction to this paper. Brunini et al. (2003) discussed the results of intra-technique comparisons between LPIM and the vertical TEC delivered to the IGS Ionospheric Working Group by the JPL (Manucci et al. 1998) and CODE (Schaer 1999). The comparisons were made for 1999, under geomagnetic conditions varying from very quiet to very disturbed (including the largest geomagnetic storm of 1999). We found a global average difference of 1.0 TECU for LPIM-CODE and 4.8 TECU for LPIM-JPL (1 TECU $\approx$ 16-cm range delay at the GPS L1

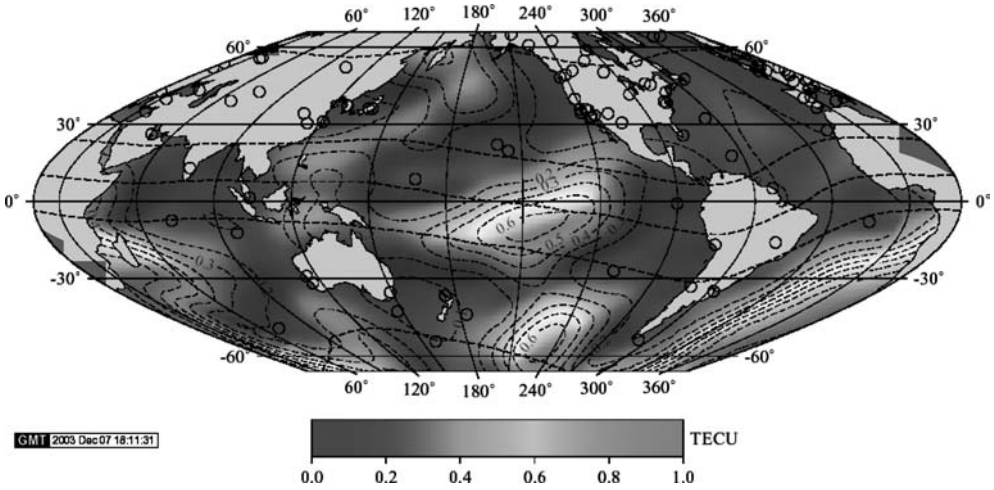

Fig. 2 Spatial distribution of the LPIM vertical TEC error after the least squares estimation (values are in TECU). The map is presented in sinusoidal projection; dashed lines represent the modified dipolar latitude equator and the ±30° and ±60° parallels; small circles depict the location of the observing GPS receivers

frequency). The discrepancies between the TEC estimates worsen during the geomagnetic storm by about 50%. We concluded that the LPIM vertical TEC is in overall agreement to the values estimated by other research groups.

2.2 Ionospheric refraction effects on T/P observations

Hereafter, $f_K = 13.6$ GHz and $f_C = 5.3$ GHz denote the frequencies of the primary and secondary T/P altimeter signals, respectively. After Chelton et al. (2001), the T/P range estimates are obtained in three steps: firstly, the individual T/P range estimates $\hat{R}(f_K)$and $\hat{R}(f_C)$ are computed from K_U- and C-band radar signals, respectively; then $\hat{R}(f_K)$ and $\hat{R}(f_C)$ are separately corrected for the SSB, which are non-random frequency-dependent range corrections; finally, the K_U-band ionospheric range delay correction is computed and removed from $\hat{R}(f_K)$. According to Chelton et al. (2001), the ionosphere-corrected range is

$$R = \tilde{R} + \tilde{\varepsilon}_R \,, \tag{1}$$

where $\tilde{R}$ is the combined range estimate from the dual-frequency altimeter

$$\tilde{R} = a_K \cdot \hat{R}(f_K) - a_C \cdot \hat{R}(f_C) \,, \tag{2}$$

and $\tilde{\varepsilon}_R$ is the combination of the errors $\hat{\varepsilon}(f_K)$ and $\hat{\varepsilon}(f_C)$ originated in both frequencies by all other sources excluding the ionosphere

$$\tilde{\varepsilon}_R = a_K \cdot \hat{\varepsilon}(f_K) - a_C \cdot \hat{\varepsilon}(f_C) \,, \tag{3}$$

where $a_K = \frac{f_K^2}{f_K^2 - f_C^2} = 1.18$ and $a_C = \frac{f_C^2}{f_K^2 - f_C^2} = 0.18$.

Using the approximate inverse relation of proportionality between the TEC and the square of the frequency, the TEC from dual-frequency range estimates $\hat{R}(f_K)$ and $\hat{R}(f_C)$ is

$$\mathrm{TEC} = \tilde{\mathrm{TEC}} + \tilde{\varepsilon}_{\mathrm{TEC}} \,, \tag{4}$$

where $\tilde{\mathrm{TEC}}$ is the combined TEC estimate from the dual-frequency altimeter

$$\tilde{\mathrm{TEC}} = \frac{a_C}{\beta_K} \cdot \left[\hat{R}(f_C) - \hat{R}(f_K) \right] , \tag{5}$$

and $\tilde{\varepsilon}_{\mathrm{TEC}}$ is the combined error

$$\tilde{\varepsilon}_{\mathrm{TEC}} = \frac{a_C}{\beta_K} \cdot \left[\hat{\varepsilon}(f_C) - \hat{\varepsilon}(f_K) \right] , \tag{6}$$

where $\beta_K = \frac{40.25 \times 10^{16}}{f_K^2} = 0.0022$ m/TECU.

From Eqs. (3) and (6), it is apparent that any range estimates error will contaminate the ionosphere-corrected range estimate, but only frequency-dependent errors will affect the TEC estimate. The sea state bias (SSB) is a frequency-dependent error (Walsh et al. 1991). Therefore, any error in the K_U- and/or C-band SSB correction will affect the TEC estimate. The SSB correction, ΔR_{SSB}, is assumed to be proportional to the significant wave height (SWH), $H_{1/3}$ (Chelton et al. 2001)

$$\Delta R_{\mathrm{SSB}} = -b \cdot H_{1/3} \,, \tag{7}$$

where b is a positive dimensionless coefficient. Typical SWH values range from about 1 m to 5 m; the lowest waves are close to the equator and the highest are in the southern subpolar ocean. The uncertainty in the SSB correction has been recognized as one of the leading sources of error in satellite altimetry. After Chelton et al. (2001), it remains at the level of about 1% of the SWH. Considering the above typical SWH values, this uncertainty can lead to errors as large as 5 cm in absolute sea-surface height and almost 5 TECU in TEC estimates.

The T/P-derived TEC dataset used in this study was provided by the Centre National d'Etudes Spatiales (CNES) through the AVISO facility (AVISO 1996). It is worth mentioning that since the launch of T/P satellite, AVISO provides an effective link between the mission and users,

ensuring quality control of data and dissemination of technical and scientific information (http://www-aviso.cls.fr). The SSB correction in the AVISO dataset was computed using the so-called parametric model. In this model, the b coefficient of Eq. (7) is formulated parametrically as a quadratic function on wind speed, U, plus a linear dependence on the SWH (Gaspar et al. 1994; Christensen et al. 1994)

$$b = a_0 + a_1 \cdot U + a_2 \cdot U^2 + a_3 \cdot H_{1/3} \,. \tag{8}$$

A different parameter set, $a_0, \ldots, a_3$, is adopted for the K_U- and C-band. The SWH and the wind speed are both obtained from the altimeter measurements. For the sake of completeness, it is also worth mentioning that Gaspar and Florens (1998) proposed a different approach to compute SSB correction, based on a non-parametric formulation of the b coefficient of Eq. (7).

3 Data processing

We compared T/P TEC estimates with vertical TEC obtained from our GPS-based LPIM and the IRI95 semi-empirical model. Depending on the performance of the IGS network, dual-frequency GPS observations from 70 to 90 globally distributed sites were used to estimate a set of spherical harmonic coefficients, describing the global vertical TEC distribution for every 2-h UT interval. Figure 2 shows the distribution of the observing sites for a typical day. The TEC derived from climatologic models like IRI is assumed to be less precise than GPS-derived TEC, because these models are intended to predict monthly average condition and quasi-periodic variation, but they lack accuracy when describing the weather of the day. In spite of this, we decided to perform comparisons against IRI95 because it provides a TEC estimate totally independent of GPS observations. We used the IRI95 software provided via ftp by the National Space Science Data Centre (NSSDC). The integration of the electron density profile was extended up to the height of the T/P satellite.

The LPIM and the IRI95 models were evaluated for the location and time of each available T/P data and the TEC biases, $B_{\mathrm{TEC}} = \mathrm{TEC}_{T/P} - TEC_{\mathrm{MODEL}}$, between T/P and the corresponding model were computed. The T/P dataset used in this paper was provided by AVISO (1996). It extends from January 1997 (T/P cycle 158) to December 1998 (T/P cycle 230) and covers a rising portion of the last solar cycle.

4 Discussion

Our initial assumption is that systematic errors of both the T/P and the LPIM TEC estimates might contribute to the TEC bias. Based on dual-frequency altimeter observations (Imel 1994), T/P provides a direct estimation of the vertical TEC over the oceans, up to a height of 1336 km. The T/P TEC might be biased by systematic errors of the model used to correct the K_U- and C-band SSB. It seems feasible that these corrections would be affected by temporal and/or spatial varying uncertainties, because a wide range of sea-state conditions are effectively ensemble-averaged into their empirical estimates. Since these corrections depend principally on the SWH (Eqs. 7 and 8), we think that any contribution of T/P to the TEC bias will be significant in those regions of large SWH.

La Plata Ionospheric Model errors may arise from several causes: systematic errors of the elevation-dependent mapping function used to convert slant into vertical TEC; omission and commission errors due to limitation of the time-dependent spherical harmonic expansion to represent the actual vertical TEC distribution; and systematic errors in the calibration of the differential code bias for the GPS receivers. We know that the contribution of LPIM to the TEC bias is large for low magnetic latitudes (Meza et al. 2002), where TEC variations are strong and fast and where the TEC distribution has large horizontal gradients. At magnetic mid-latitudes, the ionosphere is rather stable and easier to predict, thus we expect a smaller contribution of LPIM to the TEC bias at these latitudes. It is also important to bear in mind that any mis-model problem will produce worse TEC estimates in open ocean regions, where the coverage of the GPS observations is always deficient. To illustrate this problem, Fig. 2 shows the formal errors of the vertical TEC estimates by least squares, for one particular period of two hours. The contour lines in Fig. 2 show the error propagation to those regions with poor data coverage.

From the previous discussion, we conclude that the TEC bias should have a rather complex spatial and temporal varying pattern arising from the combination of errors correlated with oceans and ionosphere parameters such as SWH, wind speed, solar activity, electron distribution gradients, etc. The next sub-sections discuss the outstanding features of this pattern and attempts to separate the T/P and the LPIM contributions to the TEC bias.

4.1 Temporal variation of TEC bias for different latitudes

Our first attempt was devoted to identify a possible dependence of the TEC bias on latitude. We divided the region covered by T/P observations into ten latitudinal bands of approximately 13° width each, and computed the corresponding averages for both T/P-LPIM and T/P-IRI95 biases. The averages and their formal errors were computed assuming equally precise and uncorrelated observations. The width of the bands was chosen as narrow as possible to ensure that at least 5% of the observations would fall inside each one. From Table 1, we conclude: (a) the average bias is always positive (i.e. T/P-TEC is greater than LPIM-TEC and IRI95-TEC); (b) the bias is generally lower for LPIM than IRI95; and (c) the latitudinal variability of the biases seams to be statistically significant respect to the estimated errors.

To get an insight into the TEC variability, we plotted the time series for the different latitudinal bands and extracted their striking behaviours. Apart from the latitudinal-varying average bias previously discussed, we identified a roughly

Table 1 Average TEC biases and their errors (in TECU) for different latitudes. The number of data used for the computation is also indicated

Latitude	# Obs	TOPEX-LPIM	TOPEX-IRI95
$+52.8^\circ < \phi < +66.0^\circ$	65629	3.79 ± 0.01	4.35 ± 0.01
$+39.6^\circ < \phi < +52.8^\circ$	74984	3.13 ± 0.01	4.28 ± 0.01
$+26.4^\circ < \phi < +39.6^\circ$	87178	1.56 ± 0.01	3.44 ± 0.02
$+13.2^\circ < \phi < +26.4^\circ$	100562	2.34 ± 0.02	3.06 ± 0.03
$+0.0^\circ < \phi < +13.2^\circ$	102554	2.77 ± 0.02	2.98 ± 0.03
$-26.4^\circ < \phi < -13.2^\circ$	119502	2.62 ± 0.02	2.69 ± 0.02
$-39.6^\circ < \phi < -26.4^\circ$	139113	2.64 ± 0.01	3.91 ± 0.01
$-52.8^\circ < \phi < -39.6^\circ$	184368	4.11 ± 0.01	4.41 ± 0.01
$-66.0^\circ < \phi < -52.8^\circ$	213252	3.92 ± 0.01	4.80 ± 0.01

quadratic trend and a one-year periodic signal. In order to deal with these features, we smoothed the time series by performing a weighted moving average with a Gaussian window of 30 days' width. In this way, one smoothed value per day was computed for each latitudinal band and plotted in Fig. 3. It shows, once again, that both T/P-LPIM and T/P-IRI95 biases are mainly positive (i.e., T/P-TEC higher than LPIM- and IRI95-TEC) for all latitudes. Besides this, it is also noticeable that: (a) the LPIM values are smaller and less variable than the IRI95 values; (b) a clear annual variation can be recognized at mid-north latitudes; (c) a roughly quadratic trend is present in the equatorial and southern regions.

4.2 Temporal variation of TEC bias for different geographical regions

To perform a more detailed analysis of the temporal and spatial variability of the T/P–LPIM TEC bias, we divided the region covered by T/P observations into 985 equilateral spherical triangles with 9° sides. For every triangle, the least squares fitted a temporal-varying regression model

$$B_{\mathrm{TEC}}(t) = \alpha_0 + \alpha_1 \cdot t + \alpha_2 \cdot t^2 + \alpha_C \cdot \cos(w \cdot t) + \alpha_S \cdot \sin(w \cdot t), \quad (9)$$

where t is the time in years, $w = 2\pi/\mathrm{year}$ is the angular frequency for a seasonal signal and $\alpha_0, \ldots, \alpha_S$ are unknown coefficients to be estimated by the least squares method. The polynomial part of Eq. (9) was included to account for possible systematic errors in LPIM that behave proportionally to the TEC. This is because the intensity of the ultraviolet solar radiation (measured by the F10.7 index available at the NSSDC) grew in a roughly quadratic form, from about 60 Solar Flux Units (SFU) at the beginning of 1997, to 130 SFU at the end of 1998. Driven by the increasing solar activity, the a_{00} coefficient of the LPIM spherical harmonic expansion (the constant part of the expansion) grew in a similar fashion (a_{00} is proportional to the globally averaged vertical TEC). Accordingly, the 10-day averaged ionospheric range correction for the T/P primary frequency went down in a roughly quadratic form, from 25 mm for cycle 158, to 65 mm for cycle 230 (Ablain et al. 2004, Fig. 16). The annual signal was included in Eq. (9) to account for possible systematic errors in both LPIM- and T/P-TEC estimates, produced by seasonal changes in the sea state conditions and/or equinoxes/solstices ionospheric variability.

There are approximately 10^6 T/P data in our dataset. If they were homogeneously distributed among the 985 triangles, there would be on average 10^3 data per triangle. However, the data distribution is not homogeneous and there are triangles with less than 10^3 data. To get a reliable estimation of the coefficients in Eq. (9), we only considered those triangles with more than 250 data (25% of the average). This caused the rejection of 91 triangles (less than 10% of triangles rejected), leaving 894 usable triangles.

The goodness of the fit was evaluated applying two statistical tests. Firstly, the complete model of Eq. (9) was reduced step-by-step to smaller models, removing alternatively the seasonal, linear and/or quadratic predictors. The statistical significance level of the different predictors was evaluated applying an analysis of variance scheme based on a Fisher's test (Weisberg 1980), with a 99% confidence level. The smallest model not rejected by the test was adopted to represent the temporal variability inside each triangle. The outcome of this analysis was that the complete polynomial part of Eq. (9) was never rejected, while the seasonal signal was not significant for 225 from the 894 usable triangles. Examples of triangles with and without significant seasonal signals are shown in panels (a) and (b) of Fig. 4, respectively. The locations of these triangles are depicted in Fig. 5a. Both of them are in the low-latitude western Pacific Ocean region. The second statistical test was performed to evaluate the goodness of fit of the adopted model. It consisted of a Chi-square test (Weisberg 1980) with a significance level of 99%. No cases were rejected by this second test.

The results obtained are presented in Fig. 5. The 91 triangles rejected by the previously discussed minimum observation criterion were filled in by interpolation. Figure 5a shows the mean values for the analysed period, $\langle B_{\mathrm{TEC}} \rangle = \frac{1}{T} \sum_i B_{\mathrm{TEC}}(t_i) \cdot \Delta t_i$, T being the two-year interval from the beginning of 1997 to the end of 1998. Figure 5b shows the mean linear trends for the same period, $\langle \dot{B}_{\mathrm{TEC}} \rangle = \frac{1}{T} \sum_i \dot{B}_{\mathrm{TEC}}(t_i) \cdot \Delta t_i$, $\dot{B}_{\mathrm{TEC}}$ being the derivative with respect to time. Figures 5c and 5d respectively show the amplitudes and the phases of the seasonal signals (depicted only for those triangles where the amplitude is greater than 1 TECU; i.e. 0.16 m at L1 frequency and 2 mm at K_U frequency). Finally, Fig. 5e shows the standard deviation of the fits. To facilitate the following discussion, Fig. 5 includes the Equator and parallels at ±30° and at ±60° of modified dipolar (Modip) latitude

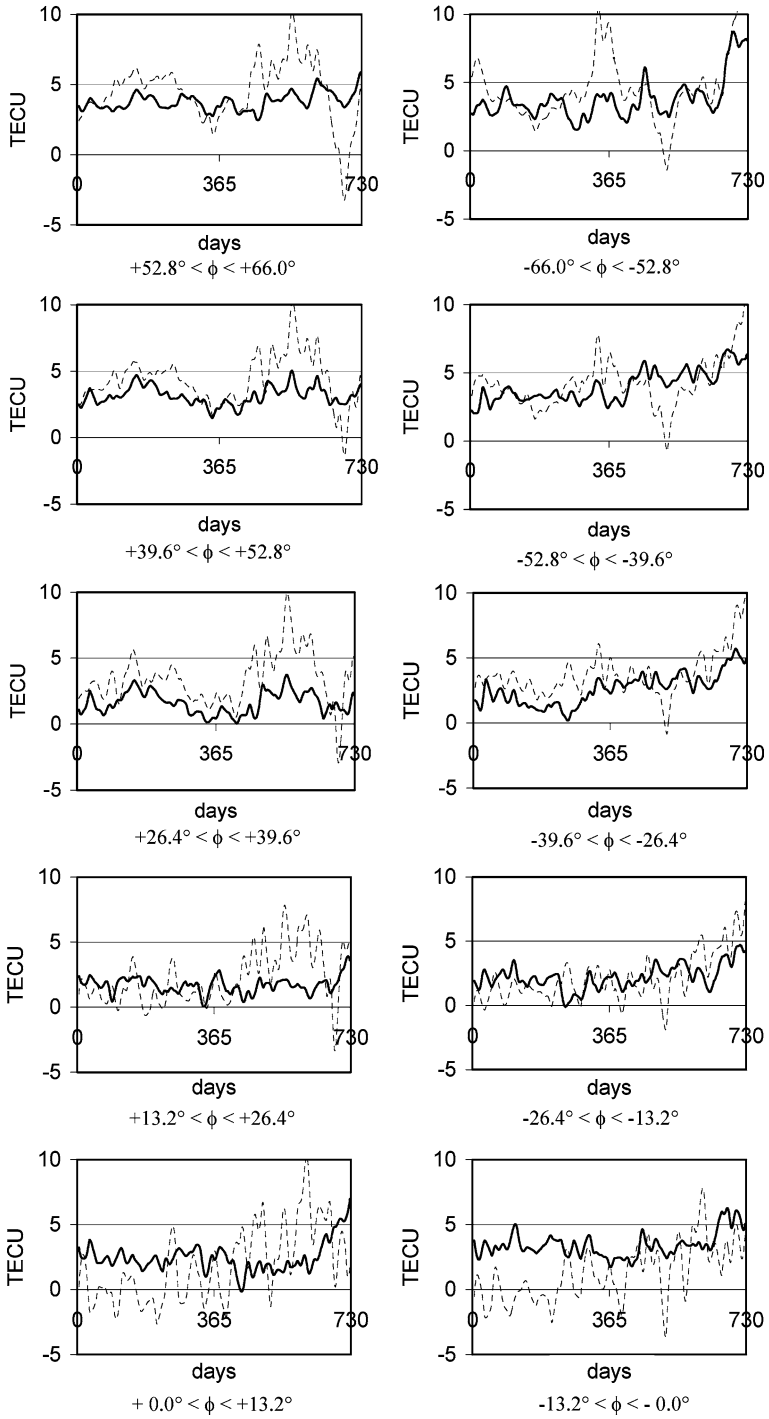

Fig. 3 Smoothed TEC bias (in TECU) for T/P–LPIM (*solid line*) and T/P–IRI95 (*doted line*); the *X*-axis shows the time (*in days*) since 1997.0.

(Rawer 1984) that roughly delimit the low- and mid-latitude ionosphere. Figure 5 shows elongated structures that delineate the well-known "camel back" shape of the equatorial anomalies, the ionospheric region where we expect the largest systematic errors of LPIM (Meza et al. 2002).

The rather high standard deviation in the anomaly region (Fig. 5e) clearly reflects the inability of LPIM to represent the strong temporal variability that characterizes the ionosphere at low magnetic latitudes. As a counterpart, equatorial oceans are characterized by rather small SWHs (Lefevre and Cotton 2001). Therefore, no large systematic errors are expected there for T/P TEC estimates. The highest waves predominate at mid-latitudes in the North Atlantic and Pacific Oceans, particularly, south of the latitude 40°S, where a broad

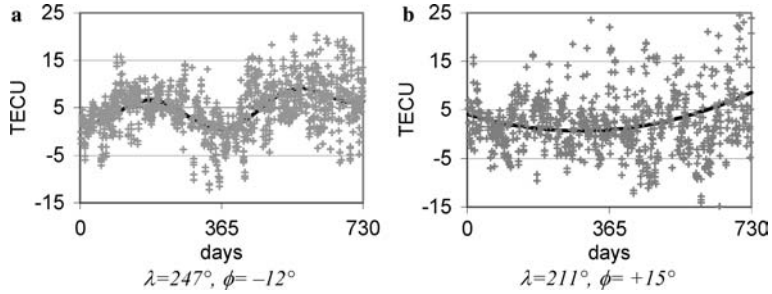

Fig. 4 Observed (*dots*) and fitted (*solid line*) T/P–LPIM TEC bias (in TECU) for triangles **a** with and **b** without significant seasonal signal; the *X*-axis shows the time (*in days*) since 1997.0

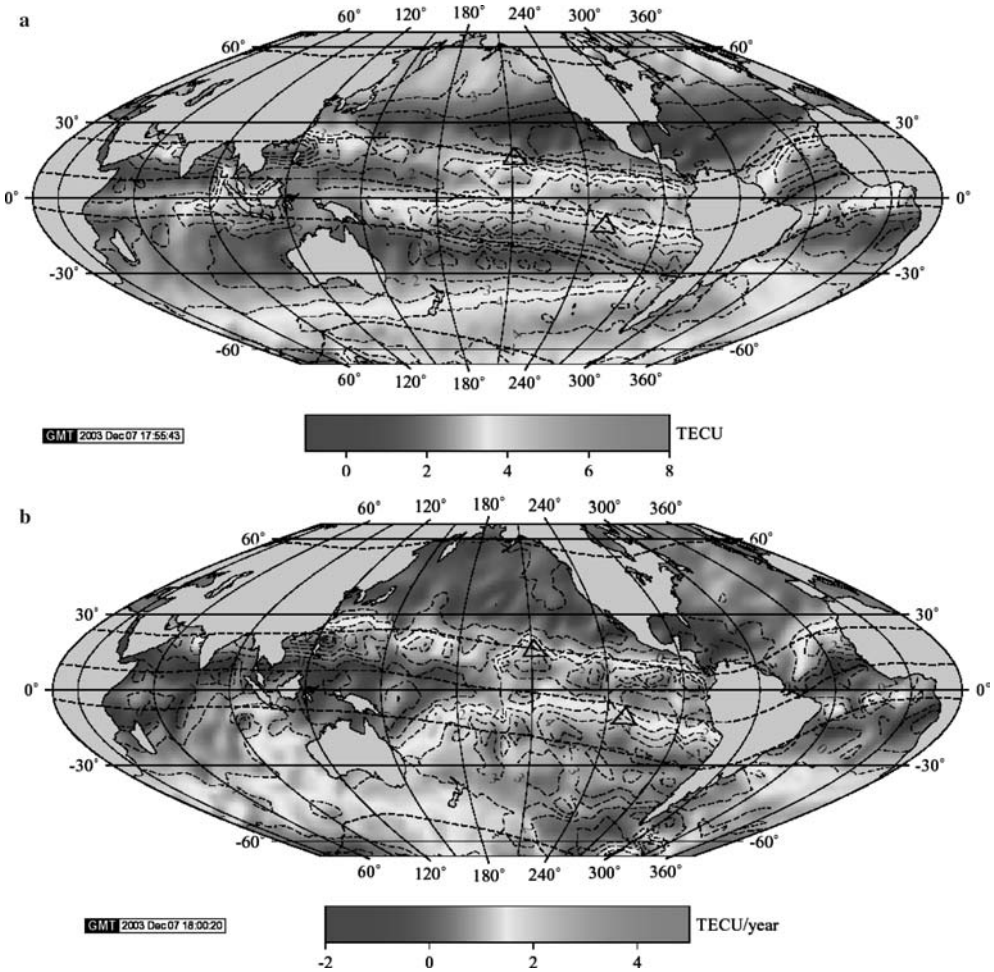

Fig. 5 T/P-LPIM TEC bias: **a** mean; **b** trend; **c** seasonal signal amplitude; **d** seasonal signal phase; and **e** standard deviation (all values in TECU, except the phase, which is in months). The maps are presented in sinusoidal projection; dashed lines represent the modified dipolar latitude equator and the $\pm 30^\circ$ and $\pm 60^\circ$ parallels

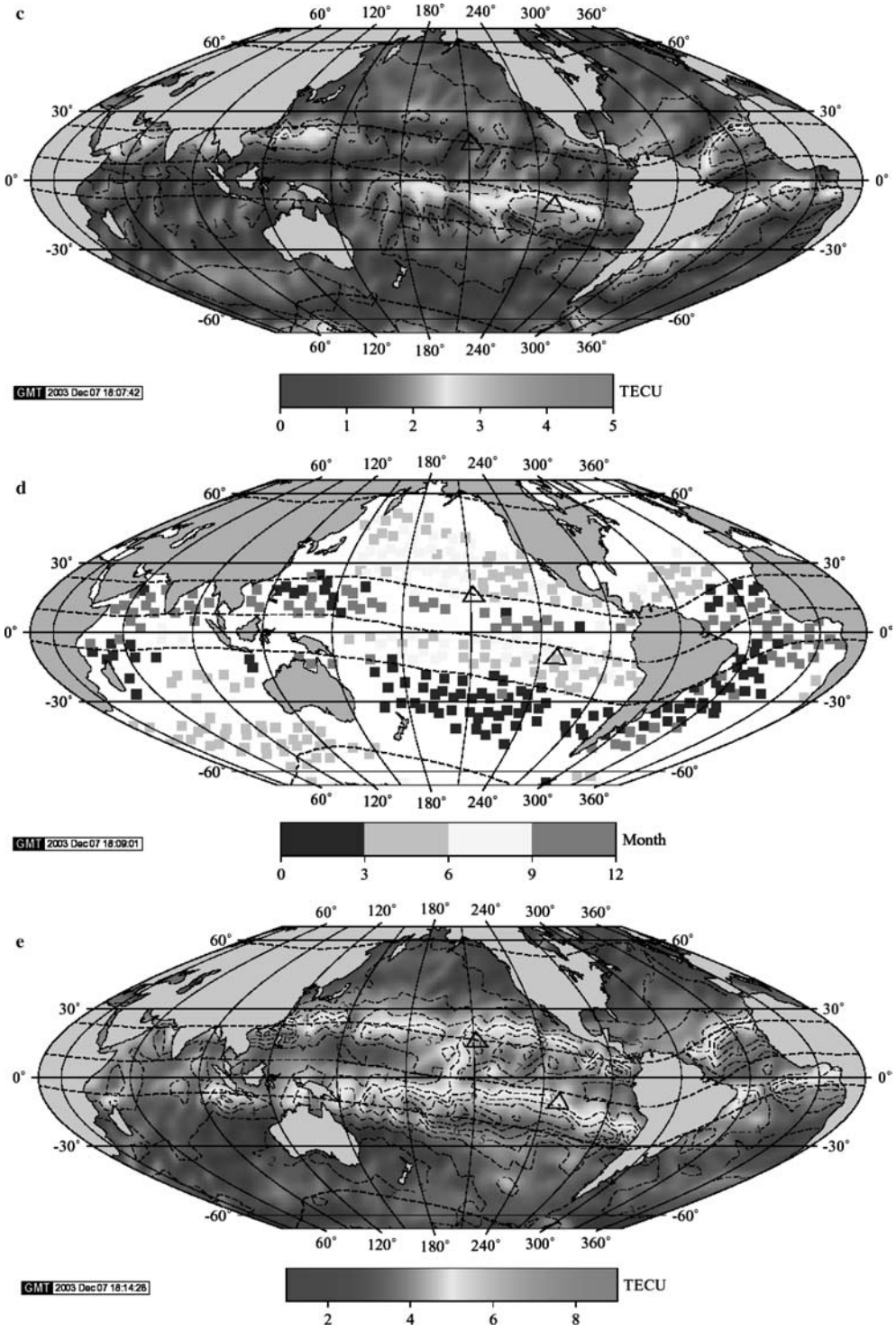
c
60° 120° 180° 240° 300° 360°
60°
30°
0°
-30°
-60°
GMT 2003 Dec 07 18:07:42
TECU
0 1 2 3 4 5
d
GMT 2003 Dec 07 18:09:01
Month
0 3 6 9 12
e
GMT 2003 Dec 07 18:14:26
TECU
2 4 6 8

Fig. 5 (Contd.)

band of high waves extend all over the longitudes. Since we do not expect large systematic errors for LPIM at mid-latitudes, the outstanding features of the TEC bias in those regions may reflect the presence of systematic errors in the SSB corrections.

The mean TEC bias (Fig. 5a) reaches the highest values, up to 4–8 TECU (0.65–1.30 m at L1 frequency, 9–18 mm at K_U frequency) in the equatorial anomalies. Beyond these anomalies, values between 3-4 TECU (0.49–0.65 m at L1 frequency, $\approx$ 7–9 mm at K_U frequency) are noticeable north and south of latitudes $\pm 40^\circ$. If we attribute this bias to a differential error between the K_U- and C-band SSB corrections, the error might range between approximately 2–5 cm (see Eq. 6). The trend (Fig. 5b) also reaches the largest values (3–5 TECU/year $\approx$ 0.49–0.81 m/year at L1 frequency, $\approx$ 7–11 mm/year at K_U frequency) in the equatorial anomalies. A region with relatively high values of 2–4 TECU/year (0.32–0.65 m/year at L1 frequency, 4–9 mm/year at K_U frequency) extends from the south equatorial anomaly (approximately –30° of Modip latitude) to –50° of geographic latitude, all over the Pacific Ocean.

This trend may be associated with the previously discussed increase of solar activity from the beginning of 1997 to the end of 1998, and could be explained by systematic errors of LPIM that are proportional to the TEC. The amplitude of the seasonal signal (Fig. 5c) shows several highlights of 2–4 TECU (0.32–0.65 m at L1 frequency, 4–9 mm at K_U frequency) along the equatorial anomalies and values greater than 1 TECU (0.16 m at L1 frequency, 2 mm at K_U frequency) at mid-latitudes regions. The phase of the seasonal signal (Fig. 5d) shows that the maximum is roughly in-phase with the local summer (September–March in the Southern Hemisphere and March–September in the Northern Hemisphere). The seasonal variation of the TEC and the SWH are, in general, in phase opposition: greater TEC and lower SWH can be expected for local summer than for local winter. We then presume that the seasonal signal described below is mostly produced by a systematic underestimation of the TEC by LPIM. Another region with amplitude greater than 1 TECU (0.16 m at L1 frequency, 2 mm at K_U frequency) is noticeable over the mid-latitude Indian Ocean, but the maximum there takes place during local wintertime. We presume that this signal is mostly due to errors in the SSB corrections rather than in the LPIM.

4.3 Temporal variation of TEC bias based on the tide gauges data

To separate systematic errors in the T/P TEC from that computed by LPIM, we used an independent information source: the T/P range bias. Moore (2001) assessed the T/P range bias by comparing sea level heights derived from T/P and from the Global Sea-level Observing System (GLOSS) tide gauge network. In that work, the altimeter range bias was computed from cycle 1 to 273, but we restricted our attention to cycles 158–230. We computed the T/P-LPIM TEC bias for those T/P observations within a radius of 150 km around the tide gauges. This radius was adopted as a compromise between: (1) to be close to the tide gauges, and (2) to have observations enough to get a reliable value. Therefore, we work with two different biases: the bias between sea-level height estimated by T/P and by tide gauges, $B_{\mathrm{SLH}} = h_{T/P} - h_{TG}$, and the TEC bias defined before, $B_{\mathrm{TEC}} = TEC_{T/P} - TEC_{\mathrm{LPIM}}$. We assume that these biases are both attributed to residual errors $\delta\Delta R_{\mathrm{SSB}}(f_K)$and $\delta\Delta R_{\mathrm{SSB}}(f_C)$ in the SSB corrections applied to the T/P range estimates and to LPIM errors, B_{MODEL}. Using Eqs. (1) and (2)

$$B_{\mathrm{SLH}} = h_{T/P} - h_{TG} = -\tilde{\varepsilon}_R = -a_K \cdot \delta\Delta R_{\mathrm{SSB}}(f_K) + a_C \cdot \delta\Delta R_{\mathrm{SSB}}(f_C), \quad (10)$$

and using Eqs. (3) and (4)

$$B_{\mathrm{TEC}} = \mathrm{TEC}_{T/P} - \mathrm{TEC}_{\mathrm{REF}} = -\tilde{\varepsilon}_{\mathrm{TEC}} + B_{\mathrm{MODEL}} = -\frac{a_C}{\beta_K} \cdot [\delta\Delta R_{\mathrm{SSB}}(f_C) - \delta\Delta R_{\mathrm{SSB}}(f_K)] + B_{\mathrm{MODEL}} \cdot \quad (11)$$

From Eqs. (10) and (11) $\delta\Delta R_{\mathrm{SSB}}(f_K)$and $\delta\Delta R_{\mathrm{SSB}}(f_C)$ can be written as functions of B_{SLH} and B_{TEC}

$$\delta\Delta R_{\mathrm{SSB}}(f_K) = -\beta_K \cdot (B_{\mathrm{TEC}} - B_{\mathrm{MODEL}}) - B_{\mathrm{SLH}}\,, \quad (12)$$

and

$$\delta\Delta R_{\mathrm{SSB}}(f_C) = -\beta_C \cdot (B_{\mathrm{TEC}} - B_{\mathrm{MODEL}}) - B_{\mathrm{SLH}}\,, \quad (13)$$

where $\beta_C = 40.25 \times 10^{16}/f_C^2 = 0.0143$ m $\times$ TECU^{-1}. The term $1 + \mathrm{a}_C = \mathrm{a}_K$ was used to derive Eqs. (12) and (13).

To analyse the TEC bias over the tide gauges, we used the same tide gauges employed by Moore (2001). Of the approximately 80 stations distributed around the world, 30% are located at geographic latitude higher than 20°, 11% are located at geographic latitude lower than 20° and 59% are located at geographic latitude between 20° and 20° (Fig. 6). For each tide gauge station, we computed the mean TEC bias

$$\bar{B}_{\mathrm{TEC}}(\varphi_i, \lambda_i) = \frac{1}{n_i} \sum_{j=1}^{n_i} B_{\mathrm{TEC_j}}\,, \quad (14)$$

where φ_i and λ_i are the latitude and longitude of the tide gauge and n_i is the total number of T/P measurement within 150 km around the tide gauge. Then, we calculated the simple average of $\bar{B}_{\mathrm{TEC}}(\varphi_i, \lambda_i)$ for every cycle, $\mu_{\bar{B}_{\mathrm{TEC}}}$, as well as its error, $\bar{\varepsilon}_{\mu_{\mathrm{TEC}}}$, from cycle 158 to 230

$$\mu_{\bar{B}_{\mathrm{TEC}}}(\mathrm{cycle}) = \sum_{j=1}^{n_{tg}} \frac{\bar{B}_{\mathrm{TEC}_j}}{n_{tg}}$$

$$\bar{\varepsilon}_{\mu_{\mathrm{TEC}}}(cycle) = \pm \sqrt{\frac{\sum_{j=1}^{n_{tg}} \left(\bar{B}_{\mathrm{TEC}_j} - \mu_{\bar{B}_{\mathrm{TEC}}}(\mathrm{cycle})\right)^2}{n_{tg} - 1}}\,, \quad (15)$$

where $n_{tg}$is the total number of tide gauges.

Figure 7a shows $\mu_{\bar{B}_{\mathrm{TEC}}}$ values (in TECU) for each cycle (solid line). Based on the results in Sect. 4.2, the following function is fitted and represented (dashed line)

$$\mu_{\bar{B}_{\mathrm{TEC}}}(\mathrm{cycle}) = a_1 + a_2 t + a_3 \cos(2\pi t) + a_4 \sin(2\pi t)\,, \quad (16)$$

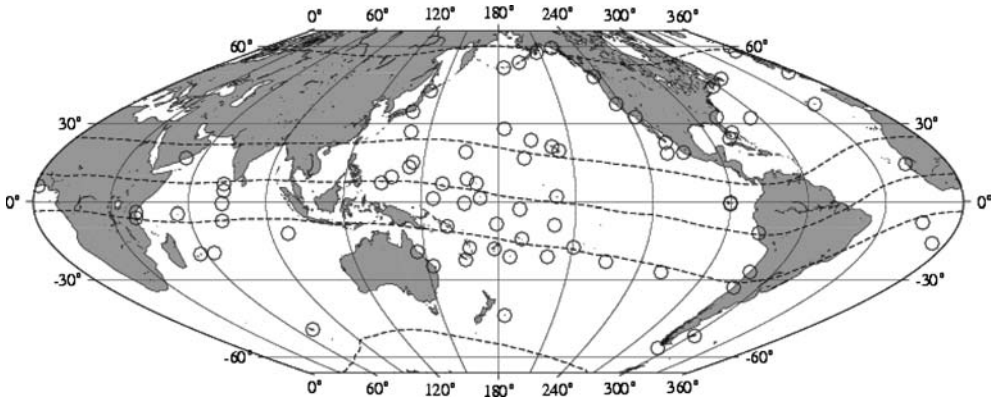

Fig. 6 Map of tide gauge locations used in the calibration of T/P (after Moore 2001)

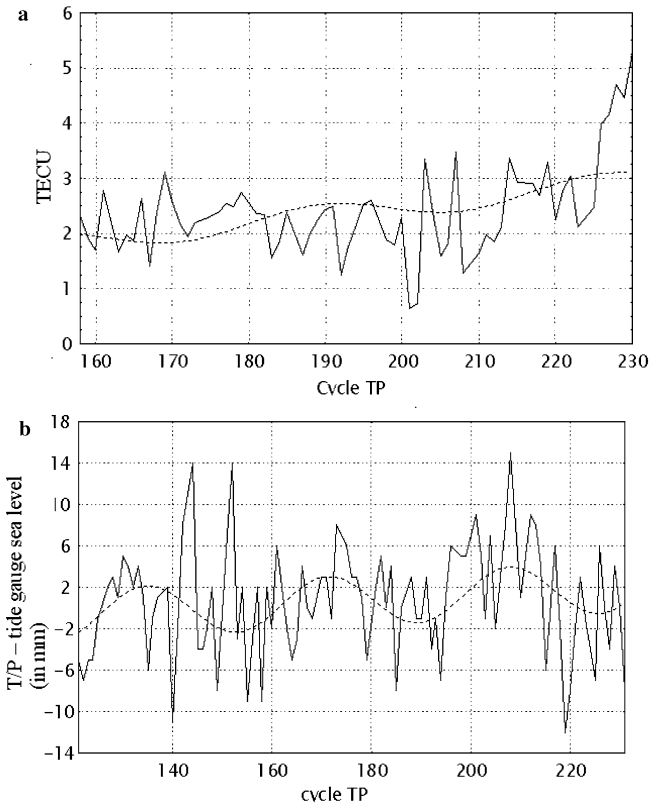

Fig. 7 **a** Simple average of B_{TEC}(in TECU) using LPIM for every cycle (*solid line*), fitted curve (*dashed line*); **b** T/P – tide gauge sea level difference (in mm) for every cycle using Moore's (2001) results (*solid line*), fitted curve (*dashed line*)

where t is the time in years since cycle 158, and $\mu_{\bar{B}_{\mathrm{TEC}}}(\mathrm{cycle})$ is given in TECU.

In Moore (2001), the altimeter range bias was obtained every cycle, $\mu_{B_{\mathrm{SLH,Moore}}}(\mathrm{cycle})$ (Fig. 7b) with an uncertainty of about 5 mm (Fig. 5, after Moore 2001). Over the same plots is fitted the function used for VTEC differences (Eq. 16). Table 2 shows the values obtained for the unknowns and their uncertainties. We evaluate the goodness of fits using a Chi-square test (e.g., Weisberg 1980) with a confidence level of significance of 99%.

Assuming that the SSB correction, ΔR_{SSB}, is proportional to the SWH, we have to take into account the SWH behaviour in K_U- and C-bands to separate the bias produced for LPIM model and for T/P measurements. Let us conjecture that the C-band SSB correction is responsible for the error in the SSB correction (Menard and Haines 2001; Ablain et al. 2004). Therefore, we may neglect the term $\mu_{\delta\Delta R_{\mathrm{SSB}}(f_K)}$, and using Eq. (11) and the values of Table 2, we obtain

$$\mu_{B_{\mathrm{TEC}}} = \frac{a_C}{\beta_K}\left(\mu_{\delta\Delta R_{\mathrm{SSB}}(f_C)} - \mu_{\delta\Delta R_{\mathrm{SSB}}(f_K)}\right) + \mu_{\bar{B}_{\mathrm{MODEL}}}$$

Table 2 Values of the unknown parameters and their uncertainties of the temporal-varying model that are fitted to the average of $\mu_{B_{\mathrm{SLH}}}$ (a_1, a_2, a_3 and a_4) and to the average of $\mu_{B_{\mathrm{TEC}}}$ (a'_1, a'_2, a'_3 and a'_4)

	a_1/a'_1	a_2/a'_2	a_3/a'_3	a_4/a'_4
$\mu_{B_{\mathrm{TEC}}}$	1.90 ± 0.99 (TECU)	0.53 ± 0.88 (TECU)	0.13 ± 0.66 (TECU)	-0.15 ± 0.71 (TECU)
$\mu_{B_{\mathrm{SLH,Moore}}}$	-0.08 ± 1.2 (mm)	1.14 ± 1.1 (mm)	-1.84 ± 0.8 (mm)	2.68 ± 0.9 (mm)

$$\mu_{B_{\mathrm{TEC}}} = \frac{a_C}{\beta_K}\mu_{\delta\Delta R_{\mathrm{SSB}}(f_C)} + \mu_{\bar{B}_{\mathrm{MODEL}}}$$
$$1.90 + 0.55\,t - 0.13\,\cos(2\pi t) - 0.15\,\sin(2\pi t)$$
$$\approx \left(\frac{0.18}{2.2}\right)\mu_{\delta\Delta R_{\mathrm{SSB}}(f_C)} + \mu_{\bar{B}_{\mathrm{MODEL}}}$$
$$\approx 0.081\mu_{\delta\Delta R_{\mathrm{SSB}}(f_C)} + \mu_{\bar{B}_{\mathrm{MODEL}}}\,. \quad (17)$$

Then, from Eq. (10) and the values of Table 2, $\mu_{\delta\Delta R_{\mathrm{SSB}}(f_C)}$ we obtain (in mm)

$$\mu_{\delta\Delta R_{\mathrm{SSB}}(f_C)} = 0 + 6.33\,t - 10.22\,\cos(2\pi t) + 14.88\,\sin(2\pi t). \quad (18)$$

From Eqs. (17) and (18), we obtain (in TECU)

$$\mu_{\bar{B}_{\mathrm{MODEL}}} = 1.90 + 0.03\,t + 0.7\,\cos(2\pi t) - 1.35\,\sin(2\pi t). \quad (19)$$

The mean C-band SSB correction error (averaged for the tide gauge network) has a secular component and an annual variability, with a maximum of 20–25 mm (about 1.4–1.8 TECU) in April–May. This seasonal signal could explain the TEC bias observed over mid-latitude Indian Ocean (Sect. 4.2). Otherwise, the mean LPIM model error has a constant and annual signal, and its maximum value is 3.4 TECU (48.6 mm at C-band) during the Southern Hemisphere summer. This is in agreement with the fact that LPIM has its worst representation in the local summer and in the Southern Hemisphere where the data coverage is poor.

An important point to take into account is that the absolute value of TEC obtained by T/P depends on the T/P altimeter calibration. This means that 3 mm as a constant term in the altimeter range bias (Eq. 16) produces a constant effect of 16.6 mm in $\mu_{\delta\Delta R_{\mathrm{SSB}}(f_C)}$ (Eq. 18), so its contribution to the constant bias in $\mu_{B_{\mathrm{TEC}}}$ would be 1.4 TECU, and $\mu_{\bar{B}_{\mathrm{MODEL}}}$ would only contribute with 0.5 TECU. We also emphasize that these results are obtained after taking an average of the differences, either of the TEC or of sea-level height, "over the tide gauges" distributed around the Earth as globally as possible (Fig. 6).

5 Conclusions

We compared vertical TEC estimates derived from T/P with the corresponding estimates derived from the IRI model and the GPS-based LPIM (Sect. 2). The comparisons were performed at a global scale (for the ocean regions covered by T/P observations) and for the years 1997–1998 (increasing solar activity). The results showed that, in general, IRI and LPIM underestimate the TEC respect to T/P. The TEC bias using LPIM is lower and less variable than using IRI. Beside this, the outstanding features of both biases are not significantly different.

The spatial and temporal variability of the TEC bias using LPIM was analysed in terms of a constant, a linear, a quadratic, and a seasonal term components. The highest values of the TEC bias delineate the equatorial anomalies. We interpret this as an indication of systematic errors mainly in the LPIM model. Among these errors, we consider that the most important are:

- Errors due to the old, but still commonly used, thin-layer ionosphere model and the mapping function used by the LPIM. The core of this approach is to assume that there is no horizontal variation of the electron distribution along the optical path of the signal from the satellite to the receiver. This approximation may worsen for the equatorial ionosphere, especially for observations at low-elevation angles and during local dusk times.
- Limitations of the time-varying spherical harmonic expansion to represent the spatial and temporal variability of the TEC in the equatorial anomaly regions. The spatial resolution of LPIM is defined by the maximum degree (12) and order (8) of the expansion. The temporal resolution is 2 h (i.e., the spherical harmonics coefficients are computed every 2 h). The relatively low degree and order of the expansion and temporal resolution can excessively smooth the peaks of the equatorial anomalies, underestimating the TEC in these regions. The spherical harmonic expansion represents the ionosphere very well at mid-latitude regions but it is less effective in the equatorial region.
- Using geographic latitude may reduce the effectiveness of LPIM to cope with the spatial and temporal ionospheric variability. It should be noted that LPIM averages the variability within each 2-h period. Moreover, to avoid unrealistic variations (including negative TEC values) in regions with poor data coverage, the expansion coefficients of consecutive periods are constrained to be the same, within a given empirical variance. These approaches might perform better if the geographic latitude were substituted for the geomagnetic or, even better, for the modified DIP latitude, because the TEC variability is smoother when it is represented as a function of these coordinates. We believe, however, that changing the latitudinal coordinate does not significantly change the conclusion of this paper. A preliminary research showed that the use of modified DIP latitude reduces the overall difference between the T/P and LPIM derived TEC by only 10%, and by less than 20% in the equatorial anomaly region (Azpilicueta F and Radicella SM, personal communication).
- Dual-frequency GPS observations provide precise determinations of the slant TEC but the accuracy strongly

depends on the calibration of the receivers' code differential biases. These biases are simultaneously adjusted with the spherical harmonic coefficients, thus suffering from any mis-model problem. It is possible that these biases absorb part of the spatial variation of the TEC for receivers located in low-latitude.
- Comparisons against T/P are performed in open ocean regions, where the coverage of GPS data is always poor.

The TEC bias using LPIM (especially the mean) also shows significant values around geographic latitude 40 °N. These are regions of rather quiet and predictable ionospheric conditions but with the highest SWH. We believe, therefore, that the TEC bias in those regions reflects some systematic error in the SSB correction model used by AVISO.

The analysis of the average temporal values of the TEC bias based on selected tide-gauge data evidences a constant bias of LPIM that produces an underestimation of the computed TEC, and the worst representation is near summer in the Southern Hemisphere. In the analysis of the residual error in the C-band SSB correction, the worst calibration problem is near winter in the Southern Hemisphere. Therefore, the TEC bias is the result of two effects: LPIM mis-modelling and T/P calibration error. Both are always present, and the bias is mostly positive due a combination of LPIM underestimation of TEC (more evident at low latitudes) and T/P altimeter calibration error (more evident at mid-latitudes).

Acknowledgements The authors are very grateful to world data centres for the free availability of the data: WDC-C, Kyoto University, Japan; Geomagnetic Information Node (GIN, British Geological Survey), Edinburgh, Scotland; N. Ness at Bartol Research Institute; CDAWeb (NASA, USA); and Scripps Institution of Oceanography from the University of California, San Diego (ftp://lox.ucsd.edu). We also thank the free availability of GMT software (Linux version).

References

Ablain M, Mertz F, Dorandeu J (2004) TOPEX/Poseidon validation activities 11 years of T/P data (GDR-Ms), CAVAL-T/P, SALP-RP-P2-EA-15161-CLS, Ramonville

AVISO/Altimetry (1996) AVISO User Handbook for Merged TOPEX/POSEIDON products, AVI-NT-02-101, Edition 3.0. Contributors are: Frédérique Blanc(*), Monique Borra, Pierrette Boudou, Sylvie d'Alessio, Philippe Gaspar, Nigel Greenwood, Christian Le Provost, Michèle Marseille, Richard Rapp, Catherine Schgounn(*), C. K Shum, Patrick Vincent

Bent RB, Llewellyn SK (1973) Documentation and description of the Bent ionospheric model. Space and Missile Organisation, Los Angeles

Beutler G, Rothacher M, Schaer S, Springer TA, Kouba J, Neilan RE (1999) The international GPS service (IGS): an interdisciplinary service in support of earth sciences. Adv Space Res 23(4):631–653

Bilitza D (1997) International reference ionosphere – status 1995/96. Adv Space Res 20(9):1751–1754

Bilitza D, Hernández-Pajares M, Juan JM, Sanz J (1999) Comparison between IRI and GPS-IGS derive electron content during 1991–97. Phys Chem Earth 24(4):311–319

Brunini C (1998) Global ionospheric model from GPS measurements. PhD Thesis, Universidad Nacional de La Plata, La Plata, Argentina

Brunini C, Van Zele MA, Meza A, Gende M (2003) Quiet and perturbed ionospheric representation according to the electron content from GPS signals. J Geophys Res 108. DOI 10.1029/2002JA009346

Chelton DB (1994) The sea-state bias in altimeter estimates of sea level from collinear analysis of TOPEX data. J Geophys Res 99:24995–25008

Chelton DB, Ries JC, Haines BJ, Fu LL, Callahan PS (2001) Satellite altimetry. In: Fu LL, Cazenave A (eds) Satellite altimetry and earth sciences. Academic, London, ISBN 0-12-269545-3, pp 57–64

Christensen EJ, Haines BJ, Keihm SJ, Morris CS, Norman RA, Purcell GH, Williams BG, Wilson BC, Born GH, Parke ME, Gill SK, Shum SK, Tapley BD, Kolenkiewicz R, Nerem RS (1994) Calibration of TOPEX/POSEIDON at platform harvest. J Geophys Res (Oceans), TOPEX/Poseidon Special Issue, 99(C12):24465–24485

Ciraolo L, Spalla P (1997) Compararison of ionospheric total electron content from the navy Navigation Satellite System and GPS. Radio Sci 32(3):1071–1080

Coco DS, Coker C, Dahlke SR, Clynch JR (1991) Variability of GPS satellite differential group delays biases, IEEE Trans Aero Elec Sys 27:931–938

Codrescu MV, Beierle KL, Fuller-Rowell TJ, Palo SE, Zhang X (2001) More total electron content climatology from TOPEX/Poseidon measurements. Radio Sci 36(2):325–333

Craven PD, Comfort RH (1988) An empirical model of the Earth's plasmasphere. Adv Space Res 8:15–24

Daniell RE, Brown LD, Anderson DN, Fox MW, Doherty PH, Decker DT, Sojka JJ, Schunk RW (1995) Parameterized ionospheric model: a global ionospheric parameterization based on first principle models. Radio Sci 30:1499–1510

Feltens J (1998) Chapman profile approach for 3-D global TEC representation. In: Dow JM, Kouba J, Springer T (eds) Proceedings of the IGS analysis centre workshop, 9–11 February, Darmstadt, pp 285–297

Fu LL, Christensen EJ, Yamarone CA, Lefebre M, Ménard Y, Dorrer M, Escudier P (1994) TOPEX/POSEIDON mission overview. J Geophys Res 99(C12): 24369–24381

Gao Y, Heroux P, Kouba J (1994) Estimation of GPS receiver and satellite L1/L2 signal delay biases using data from CACS. In: Proceedings of KIS-94, Banff, Canada, 30 August–2 September, 1994, pp 109–117

Gaspar P, Ogor F, Le Traon PY, Zanifé OZ (1994) Estimating the sea-state bias of the TOPEX and Poseidón altimeters from crossover differences. J Geophys Res 99:24981–24994

Gaspar P, Florens JP (1998) Estimation of the sea state bias in radar altimeter measurements of sea level: results from a new nonparametric method. J Geophys Res 103:15803–15814

Hernández-Pajares M (2003) Performance of IGS ionosphere TEC maps. Presented at the 22nd IGS Governing Board, Nice, 6th April 2003

Hernández-Pajares M, Juan JM, Sanz J (1999) New approaches in global ionospheric determination using ground GPS data. J Atmos Solar Terrestrial Phys 61:1237–1247

Ho CM, Wilson BD, Mannucci AJ, Lindqwister UJ, Yuan DN (1997) A comparative study of ionospheric total electron content measurements using global ionospheric maps of GPS, TOPEX radar and the Bent model. Radio Sci 32(4):1499–1512

Imel DA (1994) Evaluation of the TOPEX/POSEIDON dual-frequency ionospheric correction. J Geophys Res 99 (C12):24895–24906

Langley R (1996) Propagation of the GPS signals. In: Kleusberg A, Teunissen P (eds) GPS for geodesy. Springer, Berlin Heidelberg New York, ISBN: 3-540-60785-4, pp 103–140

Lanyi GE, Roth T (1988) A comparison of mapped and measured total ionospheric electron content using Global Positioning System and beacon satellite observations. Radio Sci 23:483–492

Lefevre J-M, Cotton PD (2001) Ocean surface waves. Chapter 7. In: Fu LL, Cazenave A (eds) Satellite altimetry and Earth sciences. Academic, New York, pp 305–328

Leitinger R, Putz E (1988) Ionospheric refraction errors and observables. In: Atmospheric effects on geodetic space measurements, Monograph 12, School of Surveying, University of New Sputh Wales, Kensington, Australia, 81–102

Manucci AJ, Wilson BD, Yuan DN, Ho CM, Lindqwister UJ, Runge TF (1998) A global mapping technique for GPS-derived ionospheric total electron-content measurements. Radio Sci 33:565–582

Manucci AJ, Iijima BA, Lindqwister UJ, Pi X, Sparks L, Wilson BD (1999) GPS and ionosphere. URSI reviews of Radio Science, Jet Propulsion Laboratory, Pasadena

Menard Y, Haines B (2001) JASON-1 CALVAL Plan, TP2-J0-PL-947-CN, CNES-JPL

Meza AM, Díaz AR, Brunini C, Van Zele MA (2002) Systematic behavior of semiempirical global ionospheric models in quiet geomagnetic conditions. Radio Sci 37(3): 9–11. DOI 10.1029/2001RS002482

Moore P (2001) The ERS-2 altimetric bias and gravity field enhancement using dual crossovers between ERS and TOPEX/Poseidon. J Geod 75:241–254

Rawer K (ed) (1984) Encyclopaedia of physics, Geophysics III, Part VII. Springer, Berlin Heidelberg New York, pp 389–391

Sardon E, Zarraoa N (1997) Estimation of total electron-content using GPS data – How stable are the differential satellite and receiver instrumental biases. Radio Sci 32:1899–1910

Schaer S (1999) Mapping and predicting the Earth's ionosphere using the Global Positioning System. PhD Thesis, Bern University

Schreiner WS, Markin RE, Born GH (1997) Correction of single frequency altimeter measurements for ionosphere delay. IEEE Trans Geosci Rem Sens 35:271–277

Walsh EJ, Jackson FC, Hines DE, Piazza C, Hevizi, McLaughlin DJ, Mcintosh RE, Swif RN, Scott JI, gel JK, Frederick EB (1991) Frequency dependence of electromagnetic bias in radar altimeter sea surface range measurements. J Geophys Res 96:20571–20583

Weisberg S (1980) Applied linear regression. Wiley , New York, ISBN 0-471-04419-9

Zlotnicki V (1994) Correlated environmental corrections in TOPEX/POSEIDON, with a note on ionospheric accuracy. J Geophys Res 95:2899–2922